15-LA-523-INMM

MEASUREMENT ISSUES WITH RADIOACTIVE WASTE DRUMS CONTAINING HETEROGENEOUS MATRICES AND NON-UNIFORM ACTIVITY DISTRIBUTIONS

John A. Mason and Marc R. Looman
ANTECH, A. N. Technology Ltd.
Unit 6, Thames Park, Wallingford, Oxfordshire, OX10 9TA, England

ABSTRACT

In both nuclear safeguards measurements and radioactive waste assay, measurement errors arise and are often undetected. Perhaps the most significant cause of such errors is a lack of knowledge of the material being measured and the consequent inappropriate choice of measurement method. The two factors, which are the dominant sources of error in safeguards and waste measurement, are matrix heterogeneity and the non-uniform distribution of activity in the measured sample. In order to appreciate the contribution made by these factors, the measurement of a variety of radioactive materials and matrices in 200 litre (55 gallon) drums have been modelled using benchmarked MCNP Monte Carlo models. Simulated measurements have been performed for drums with homogeneous matrices with uniform density and activity distribution for a range of density values. These results have been compared to the results of simulations where both drum matrix and activity distribution are non-uniform. The Far Field measurement method has been employed in the simulations. It is the simplest measurement process and is based on the assumption of drum uniformity. As a result, Far Field measurements exhibit the largest measurement errors due to heterogeneity in matrix and activity distribution. Other measurement technologies have been developed to reduce the measurement errors that arise from matrix heterogeneity and non-uniform activity distribution. These measurement technologies include both segmented gamma scanning and tomographic gamma scanning. The reductions in measurement errors using these alternate measurement methods are also considered.

INTRODUCTION

Benchmarked MCNP Monte Carlo simulations [1] for drum measurements using a high purity Germanium (HPGe) detector have been performed. The purpose is to illustrate the significance of measurement errors, which are due to matrix heterogeneity and the non-uniform distribution of activity in drums containing radioactive material. Simulations of drums with uniform matrices and activity distributions are employed as a reference and the results are quoted in terms of normalized detection efficiency. Separate simulations have been performed in which either the matrix or the activity distribution is heterogeneous while the other characteristic remains uniform. In a final case both the matrix and activity distribution are heterogeneous. The normalised results are compared with the results of the uniform reference cases. This is accomplished by comparing the equivalent normalized detection efficiencies where all other parameters such as density and activity are equivalent. For example, the total source activity is the same when comparing cases with uniform distributed activity and with point sources.

The simulated measurements are Far Field (sometimes called “one shot”) measurements where the entire drum envelope is in the field of view of the collimated HPGe detector and the drum is rotated to reduce errors resulting from matrix or activity distribution radial inhomogeneity. The HPGe detector obtains a single gamma ray spectrum and the drum average density is determined from the drum weight.

There are several Far Field measurement codes such as the ANTECH ISOCorr™ far field geometry spectroscopic analysis code [2]. ISOCorr is functionally equivalent to other Far Field analysis codes such as ISOCS™, ISOTOPIC™ and SNAP™. Although detailed implementations differ, the operation of all of these codes is based on the assumptions that the matrix material in the drum is uniform - of a constant density and composition and that the radioactivity is uniformly distributed throughout the drum. This implies that every volume element (or voxel) in a drum has the same activity and matrix density and hence the same gamma ray attenuation. In the analysis process, the activity contribution or amount of radioactivity in each voxel is summed (taking into consideration matrix attenuation) to calculate the total activity in the drum. Assessing the magnitude of the errors that arise when these assumptions are violated is the purpose of the analysis described in this paper.

BENCHMARKING THE MONTE CARLO MCNP SIMULATIONS

The simulated measurements are based on the modelling of a real measurement system, the ANTECH Far Field Gamma Monitor [2]. The MCNP model benchmarking process utilises a collimated AMETEK/ORTEC GEM-F7040P4 Profile F-Series HPGe detector with a nominal efficiency of 40% and three NIST traceable calibrated gamma sources. For the three sources, Ba-133, Cs-137 and Eu-152, the radioactive material is located in a 1 mm diameter epoxy bead, which is placed centrally in a low attenuation encapsulation PMMA plastic disk, 3 mm thick and 25.4 mm diameter. The disk is positioned on the detector axis at a distance of 50 cm from the detector aluminium window. Although the attenuation by the plastic source is small, and about 1.5 % for the 662 keV gamma rays from Cs-137, the MCNP model includes the epoxy bead and the PMMA disk.

In order to obtain agreement between the experiment and the simulation for all the main gamma rays of the three sources it is necessary to adjust the outer dimensions of the germanium crystal and the thickness of the dead-layer in the model. The origin of this necessity may be attributed to imperfect charge collection at the extremities of the germanium crystal. We have also found that the thickness of the dead-layer reported in the manufacturers Quality Assurance Data Sheet (QADS) does not always correspond to the optimum thickness obtained from the simulation. The results from the parameter study are listed below. All other detector parameters are those from the QADS.

- Crystal Diameter 68.4879 mm (QADS value is equal to 69.9 mm)
- Crystal Length 42.9 mm (QADS value is equal to 43.3 mm)
- Dead Layer Thickness 0.70 mm (QADS value is equal to 0.7 mm)

The results of the comparison between measurement and simulation are presented in Table 1 and Figure 1. Note that the overall agreement is very good for the “tuned” crystal model even though the uncertainty of the activity of the sources is 3% as reported in the calibration certificates. The measured results for gamma-rays from Ba-133 and Cs-137 are in good agreement with those from Eu-152 and the simulation results, giving another indication of the high quality of the benchmark.

Energy (keV)	EXP		SIM		SIM/EXP	
	Value	Rel. Error	Value	Rel. Error	Value	Rel. Error
40.1	7.896E-05	0.036	7.953E-05	0.013	1.007	0.039
81.0	6.833E-04	0.031	6.714E-04	0.004	0.983	0.031
121.8	8.213E-04	0.030	8.070E-04	0.004	0.983	0.030
244.7	6.116E-04	0.031	6.179E-04	0.005	1.010	0.031
276.4	5.581E-04	0.031	5.602E-04	0.005	1.004	0.031
302.9	5.153E-04	0.030	5.172E-04	0.005	1.004	0.031
344.3	4.660E-04	0.034	4.624E-04	0.005	0.992	0.034
356.0	4.493E-04	0.030	4.490E-04	0.005	0.999	0.031
383.9	4.183E-04	0.031	4.190E-04	0.006	1.002	0.031
661.7	2.651E-04	0.030	2.619E-04	0.007	0.988	0.031
778.9	2.312E-04	0.031	2.289E-04	0.008	0.990	0.032
867.4	2.080E-04	0.037	2.104E-04	0.008	1.012	0.037
964.1	1.920E-04	0.034	1.932E-04	0.008	1.006	0.035
1112.1	1.712E-04	0.031	1.715E-04	0.009	1.002	0.033
1408.0	1.420E-04	0.031	1.424E-04	0.010	1.002	0.032

Table 1. *Detection efficiency results from experiment (EXP), simulation (SIM) and their ratio for the main gamma-rays of the Ba-133, Cs-137 and Eu-152 calibrated sources. The errors are relative errors with a 95 % confidence interval (2σ). The errors for the simulation are for statistical uncertainty only. The errors for the experiment are dominated by the 3% uncertainty of the activity as reported in the calibration certificates, which are slightly increased due to counting uncertainty.*

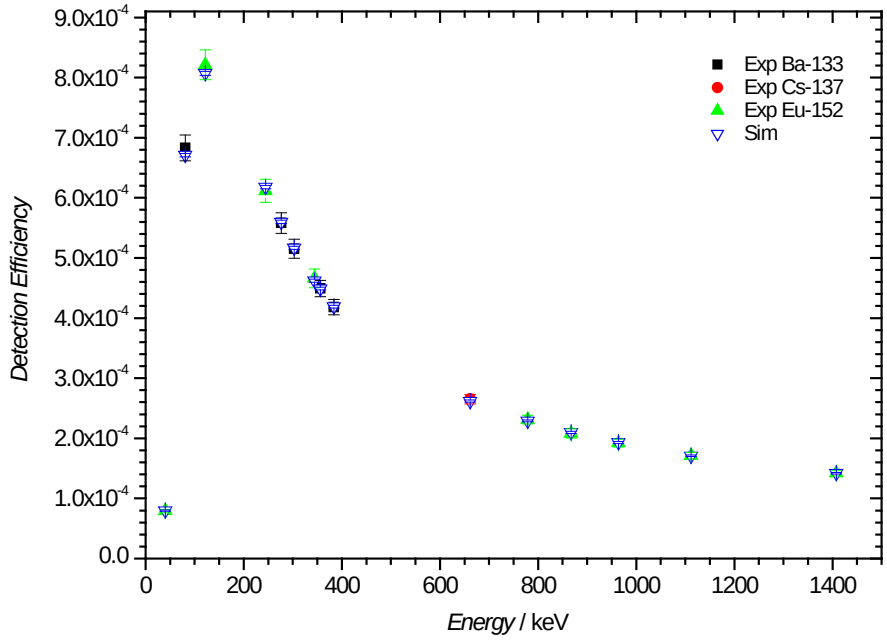

Figure 1. *Measured and simulated detection efficiency as a function of energy.*

Figures 2 and 3 show respectively the horizontal and vertical sections of the MCNP model. Note that the aperture of the collimator is smaller than in conventional far field systems. This smaller width is to reduce the number of background counts, resulting in an improvement of the Minimal Detectable Activity (MDA). The fraction of the gamma-rays emitted by the drum that are blocked by the collimator is negligible. The collimator has a build in automated filter for the measurement

of hot or high activity drums. The filter has 3 positions: no filter, 15 mm tungsten filter and 30 mm tungsten filter. The filters are not used or considered further in the present analysis.

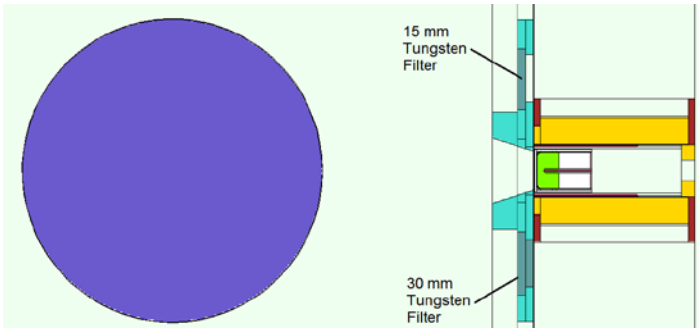

Figure 2. *Horizontal section through centre of drum, Z = 43.05 cm.*

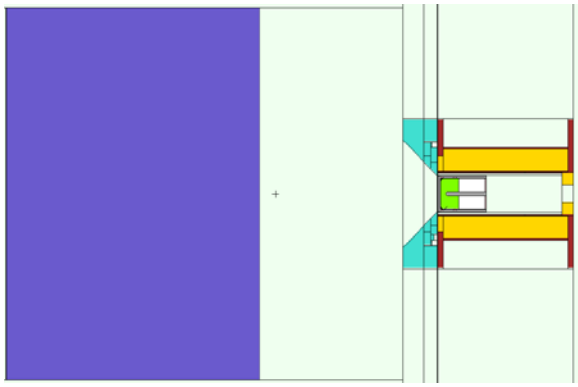

Figure 3. *Vertical section through centre of drum, Y = 0 cm.*

A detailed view of the detector model is given in Figure 4. The detector is positioned at the half height of the inner height of the 200-litre drum (Z=43.05 cm). The inner drum volume starts at 1.6 cm from the bottom of the drum, which coincides with Z=0. The inner diameter of the drum is equal to 57.2 cm, and the inner height is equal to 82.9 cm. The thickness for the steel wall of the drum is equal to 1 mm, and is the same for the top, bottom, and wall of the drum. The distance between the centre of the drum and the front window of the detector is equal to 69.1 cm (the space between drum outer surface and detector window measures 40.4 cm). The characteristics of the drum matrices are given in Table 2, the densities for the air, sawdust, water and sand are respectively 1.21E-03, 1.44E-01, 1.00E+00 and 1.58E+00 g·cm^{-3}.

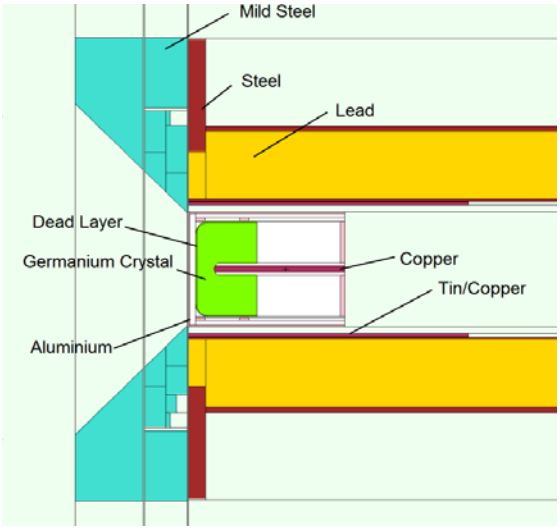

Figure 4. *Vertical section through centre of the detector crystal.*

Table 2. *Atom fractions of the drum matrices of interest.*

Atom	Air	Sawdust	Water	Sand
H	4.14E-06	4.95E-01	6.67E-01	
He	2.63E-06			
C	1.99E-04	2.57E-01		
N	7.84E-01			
O	2.11E-01	2.48E-01	3.33E-01	6.67E-01
Ne	9.13E-06			
Si				3.33E-01
Ar	4.69E-03			
Kr	5.72E-07			

SIMULATION RESULTS FOR DIFFERENT DRUM MATRICES AND SOURCE DISTRIBUTIONS

A number of simulated drum measurements have been made in order to assess the errors that arise from using Far Field analysis with heterogeneous drums. Four matrices are employed (air, sawdust, water and sand) which cover a range of density of materials commonly encountered. Three gamma ray energies (59.5 keV, 661.7 keV and 1332.5 keV) corresponding to the radionuclides Am-241, Cs-137 and Co-60 have been used in the analysis.

Volume Sources in Homogeneous Matrices

For comparison the initial measurement simulations are of drums of varying density and matrix content but with uniform source distributions and uniform matrices. The resulting normalised measurement detection efficiencies that are determined in the simulations are used as a basis of comparison so the deviations or measurement errors arising from using the far field method to measure heterogeneous drums may be identified. The detection efficiencies for homogenous activity distribution and homogenous matrix are reported in Table 3. In the simulation the photons are emitted isotropically. Normalised detection efficiencies are used to facilitate comparisons in the remainder of the paper.

Case	Matrix	Energy (keV)	Efficiency		
			Value	Error (2σ)	Error %
1	Sand	59.5	6.20E-06	2.03E-07	3.3
2	Sand	661.7	2.42E-05	4.03E-07	1.7
3	Sand	1332.5	1.92E-05	3.57E-07	1.9
4	Water	59.5	1.30E-05	2.93E-07	2.3
5	Water	661.7	3.29E-05	4.68E-07	1.4
6	Water	1332.5	2.53E-05	4.10E-07	1.6
7	Sawdust	59.5	5.06E-05	5.76E-07	1.1
8	Sawdust	661.7	9.47E-05	7.96E-07	0.8
9	Sawdust	1332.5	5.95E-05	6.30E-07	1.1
10	Air	59.5	7.08E-05	6.94E-07	1.0
11	Air	661.7	1.22E-04	9.05E-07	0.7
12	Air	1332.5	7.16E-05	6.87E-07	1.0

Table 3. *Efficiencies for uniform volume sources in homogeneous matrices.*

Point Sources in Homogeneous Matrices

A source of error in Far Field measurements arises when the source distribution is not homogenous. The worst-case scenario occurs when all the activity is located in a single position, i.e. in a point source. In the MCNP simulations a point source is modelled as a ring, since the drum is rotated during the measurement. Figures 5 to 8 give the results for simulated measurements of point sources at various radial positions, for the selected energies and matrices. Each curve is normalised against the detection efficiency for the corresponding volume source calculation (see Table 3). Note that the point source activity is the same value as the distributed source activity for the corresponding calculations of uniform volume sources in homogeneous matrices (see Table 3).

The results displayed in Figures 5 to 8 are broadly similar. For the low-density matrices of air and sawdust where there is relatively low attenuation, the errors are small and the effects of geometry dominate the curves. Large and potentially very large errors occur where there is higher density and hence significant attenuation. In all cases increasing gamma ray energy reduces the attenuation effect and reduces the errors. For 60 keV gamma rays from Am-241, the errors are very large compared to a uniform distributed source of the same value: a factor of more than 1000 for point sources near the drum centre and greater than a factor of 4 for a point source on the drum periphery. Clearly in these cases using far field measurements will often lead to large errors.

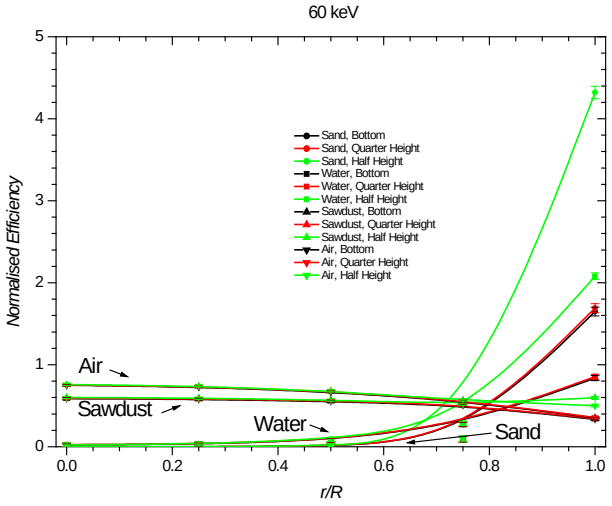

Figure 5. *Normalised detection efficiency as a function of the radius fraction for gamma-rays with an energy of 60 keV (R is the inner radius of the drum).*

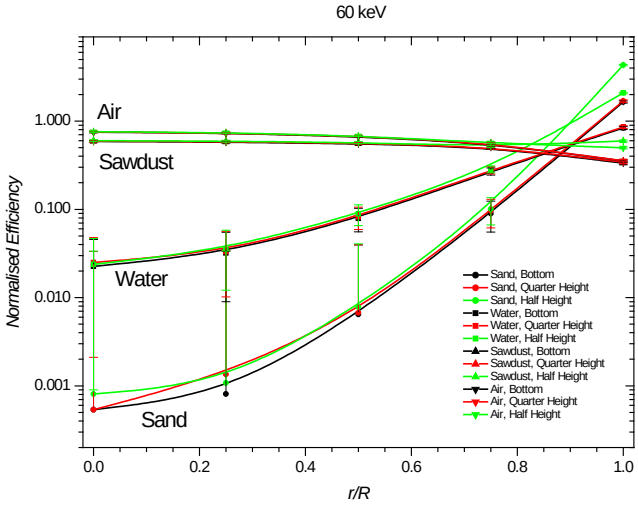

Figure 6. *As previous plot but with logarithmic scale.*

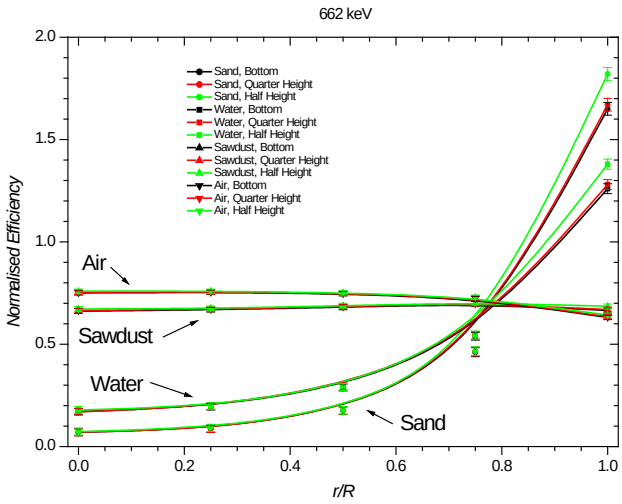

Figure 7. *Normalised detection efficiency as a function of the radius fraction for gamma-rays with an energy of 662 keV (R is the inner radius of the drum).*

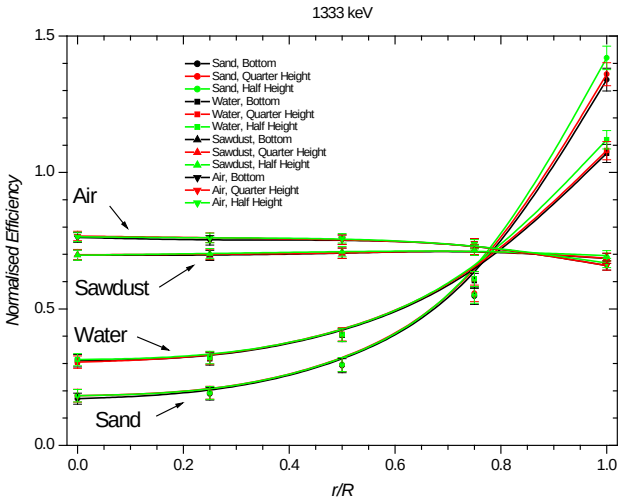

Figure 8. *Normalised detection efficiency as a function of the radius fraction for gamma-rays with an energy of 1333 keV (R is the inner radius of the drum).*

Homogeneous Volume Source in Non uniform Matrices

We now consider the reverse situation where the activity distribution is uniform but the matrix density is heterogeneous. The inner volume of the drum is split into 6 regions of equal volume (see Figure 9). The density of adjacent regions is varied; one is assigned a density below the nominal density and the other a density above nominal. The overall (average) density of the drum is equal to that of the volume source cases.

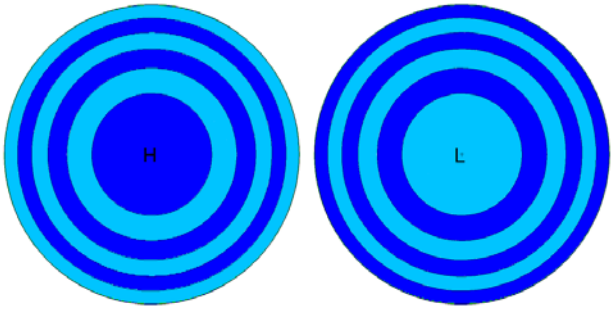

Figure 9. *Geometries of the two scenarios used for the non-homogenous matrix cases. The lighter and darker colours indicate respectively regions with lower and higher densities. On the left is shown the geometry for the cases labelled with (H) in Figures 10 to 12, whereas on the right the geometry for the cases labelled with (L) is shown (the letter indicates the density of the central region).*

Density Variation (%)	Sawdust		Water		Sand	
	L	H	L	H	L	H
0	0.144		1.000		1.579	
20	0.115	0.173	0.800	1.200	1.263	1.895
40	0.087	0.202	0.600	1.400	0.948	2.211
60	0.058	0.231	0.400	1.600	0.632	2.527
80	0.029	0.259	0.200	1.800	0.316	2.842
100	0.000	0.288	0.000	2.000	0.000	3.158

Table 4. *Densities in $g \cdot cm^{-3}$ used in the simulation for the low density and high density zones for sawdust, water and sand matrices and for various degrees of density variation.*

Figures 10 to 12 display the results in terms of normalised efficiency as a function of increasing density variation. As before the corresponding homogeneous case has an efficiency of one.

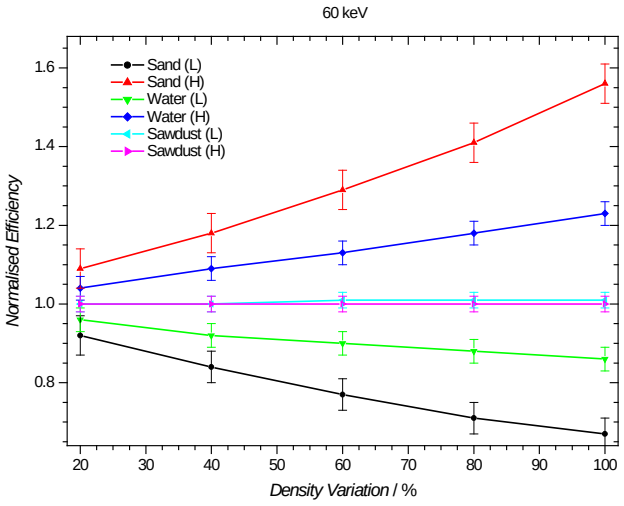

Figure 10. *Normalised detection efficiency as a function of the density variation in percent for gamma-rays with an energy of 60 keV.*

The low density matrices with low attenuation show almost no effect as the density variation is increased. As expected, the effect is reduced as the gamma ray energy increases. Significant errors arise, however, for higher density matrices and lower energy gamma rays. In Figure 10, errors of nearly 60% are observed. Very large errors will arise for matrices with even larger variations in density and such variations are not uncommon in real waste drums.

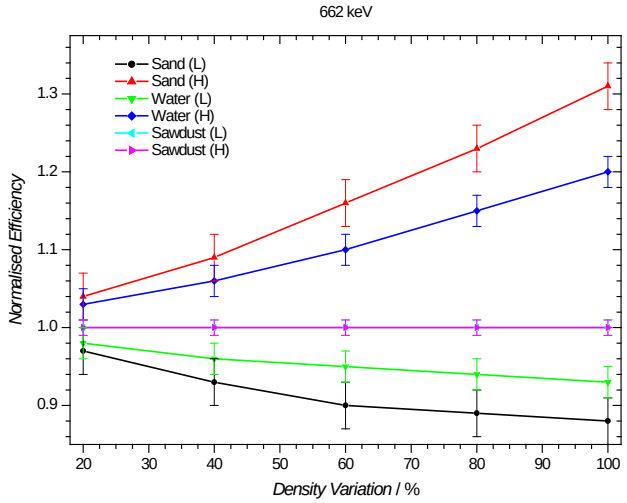

Figure 11. *Normalised detection efficiency as a function of the density variation in percent for gamma-rays with an energy of 662 keV.*

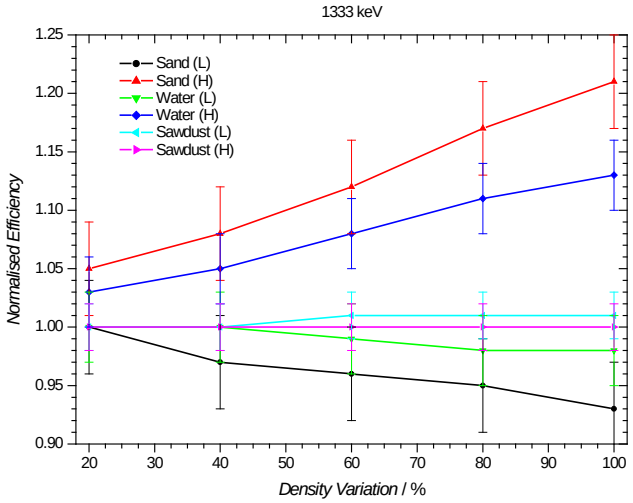

Figure 12. *Normalised detection efficiency as a function of the density variation in percent for gamma-rays with an energy of 1333 keV.*

Point Source in a Heterogeneous Matrix

A final example includes both heterogeneity in the matrix and radioactive source distribution. In this example a steel slab is located inside a drum within a sawdust matrix. Two cases with equal slab dimensions of 10.16 x 5.08 cm but with different thickness, i.e. 2.54 cm (1 inch) and 5.08 cm (2 inches) have been considered. A point source is located on the surface of the steel slab simulating radioactive contamination on a component in a drum of mixed waste. The steel slab provides shielding reducing the signal from the source as seen by the HPGe detector (Figures 13 and 14).

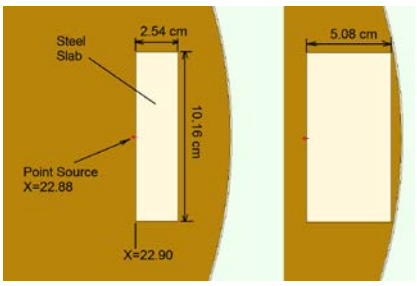

Figure 14. *Position of the steel slabs for 2.54 cm thick slab (left) and 5.08 cm thick slab (right). The source is placed just behind the slab (X = 22.88 cm = 0.8 R).*

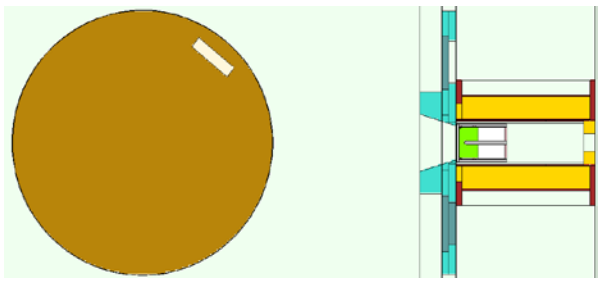

Figure 13. *A rotation angle of 50° yields minimal efficiency due to the combined effect of increased detector distance and a longer path through the slab.*

Normalised detection efficiencies for these two examples for both Cs-137 and Co-60 gamma ray energies are plotted as a function of drum rotation angle in Figure 15.

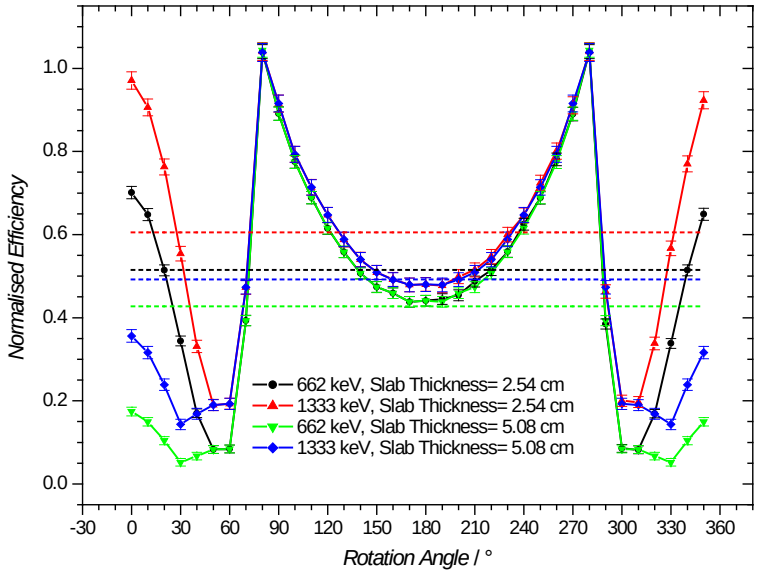

Figure 15. *Normalised detection efficiency as a function of rotation angle in degrees for photon with energies of 662 and 1333 keV and for steel slab thickness of 2.54 and 5.08 cm. The dashed lines correspond to the average results over a 360° rotation.*

Figure 15 shows the significant variations of normalised detection efficiency as the drum is rotated. The simulated measurement result is the average normalised detection efficiency. These are plotted as dashed lines for the two slab thicknesses and two gamma ray energies. The normalised efficiencies are tabulated in Table 5. For these relatively benign cases the measurement errors range from 40% to almost 60% compared to the corresponding uniform reference cases.

Slab Thickness (cm)	Energy (keV)	Normalised Efficiency		
		Volume Source	Point Source Without Slab	Point Source With Slab
2.54	662	1.000	0.700	0.515
2.54	1333	1.000	0.711	0.605
5.08	662	1.000	0.700	0.427
5.08	1333	1.000	0.711	0.492

Table 5. *Normalised detection efficiencies (average results for a 360° rotation) for photons with energies of 662 and 1333 keV and for steel slab thickness of 2.54 and 5.08 cm.*

CONCLUSIONS

The simulated far field measurement data that has been presented shows that the far field measurement process can result in large and undetermined errors when the assumptions of matrix homogeneity and uniformity of source distribution are violated in a significant way. The simulated examples that have been considered in the paper are relatively benign. In reality, measurement errors of greater than a factor of 10 are not uncommon and have been observed by the authors in measuring real waste drums and containers.

In order to address some of the limitations of the Far Field method other measurement techniques such as the SGS [3] and TGS have been devised. In an SGS measurement the drum is measured in vertical segments and a transmission correction for attenuation is made for each separate vertical segment. Rather than assuming that the entire drum has a uniform matrix and source distribution, an SGS measurement [4] assumes only that each segment is uniform but each segment can have a different activity and different density. Use of an SGS in place of the Far Field method will significantly reduce measurement errors and avoid excessively conservative measurements of activity. In appropriate cases, a TGS instrument is capable of providing even more accurate results as it determines the unique individual attenuation and activity for each volume element throughout the drum matrix. The applicability of the TGS is generally limited to measurements of drums of relatively low density or high source strength due to significant limitations in counting statistics and measurement time. In general the SGS technique provides a good compromise considering sensitivity, accuracy and measurement time.

HPGe detectors employed in both Far Field and SGS instruments are calibrated for gamma ray energy and detection efficiency with traceable point sources. However, in their analysis both methods assume that in the former case the drum has a uniform matrix and source distribution and in the latter case that the drum segment has a uniform matrix and source distribution although each segment may have a different attenuation and activity. Clearly in view of the results presented in this paper, it is inappropriate to perform calibration verification of both Far Field and SGS instruments with point sources. In the same way that a point source can be modelled using MCNP in a rotating drum by a ring source, in a real measurement, typically 6 rod sources of equal activity placed in equal radial volumes of a rotating drum and spaced in a helical configuration provide a close approximation to a real radioactive drum with a uniform distributed source. This approach has been used successfully to perform calibration verification in matrices of different density for both Far Field [2] and SGS [4] instruments.

The authors wish to thank Dr E. Ray Martin for useful discussions.

REFERENCES

[1] J. F. Briesmeister, *MCNP - A General Monte Carlo N-Particle Transport Code (Version 4C)*, Los Alamos National Laboratory, LA–13709–M, 2000.

[2] Marc R. Looman, Erik Lindberg, E. Ray Martin, John A. Mason, Lawrence V. Odell, Matt Piotrowski, Adam Poundall, Antony C. N. Towner and Zhang Wei, *"Design and Performance Testing of a Novel Far Field Gamma System to Assay Radioactive Waste in 400 and 200 litre Drums"*, WM2015 Conference, March 15–19, 2015, Phoenix, Arizona, USA. (WM15-15339)

[3] E. R. Martin, D. F. Jones, and J. L. Parker, *Gamma Ray Measurements with the Segmented Gamma Scan*, Los Alamos Scientific Laboratory, LA-7059-M, 1977.

[4] J. A. Mason, M. R. Looman, E. R. Martin, L. V. Odell, M. Piotrowski, Adam Poundall, William Tansey and A. C. N. Towner, "*Design, Development and Testing of an Automated Segmented Gamma Scanner for Measuring Nuclear Power Station Radioactive Waste*", Proceedings of INMM15, Indian Wells, CA, July 2015. (15-A-473-INMM)